DOI: http://doi.org/10.4038/jgssl.v22i2.67 *Journal of Geological Society of Sri Lanka Vol. 22-2 (2021), 1-14*

METAMICT FERGUSONITE FROM KOLONNA AND MASIMBULA, SRI LANKA

A. ERLACHER[1], M. ZEUG[1], R. ŠKODA[2], K.A.G. SAMEERA[3,4] , L. NASDALA[1*]

[1] *Institut für Mineralogie und Kristallographie, Universität Wien, Althanstr. 14, A–1090, Wien, Austria*
[2] *Department of Geological Sciences, Faculty of Science, Masaryk University, Kotlářská 267/2, 61137 Brno, Czech Republic*
[3] *Geological Survey and Mines Bureau, 569 B120, Sri Jayawardenepura Kotte 10100, Sri Lanka*
[4] *Postgraduate Institute of Science, University of Peradeniya, P.O. Box 25, Peradeniya 20400, Sri Lanka*

[*] *Corresponding author: lutz.nasdala@univie.ac.at*

(Received 22nd November 2021; accepted 17th December 2021)

ABSTRACT

Two radioactive mineral specimens (with compositions ThO_2 2.9–4.6 wt% and UO_2 5.8–7.8 wt%, respectively), collected from a placer deposit near Kolonna and a quarry near Masimbula, Sri Lanka, were identified as metamict fergusonite. Identification was based on samples' chemical compositions and the observation that both specimens were transformed to crystalline fergusonite upon dry annealing at 550–600 °C, including the spectroscopic observation of a high-temperature $\alpha \rightarrow \beta$ transition (≥750 °C) that is characteristic of this mineral. Strong negative Eu anomalies in chondrite-normalised REE patterns indicate reducing formation conditions. Both samples have experienced (perhaps even multiple) chemical alteration processes that led to the formation of decidedly heterogeneous internal textures. Fluid-driven alteration, especially along fractures and domain boundaries, has resulted in vast chemical changes.

Keywords: *Fergusonite–(Y), Radioactivity, Metamict, Annealing, Raman spectroscopy*

1. INTRODUCTION

Apart from common and rare gem minerals, placer deposits in Sabaragamuwa province of Sri Lanka typically contain significant fractions of rather unattractive, heavy and radioactive minerals of dark colour, which are often referred to as "*katta*". Among those, the occurrence of fergusonite (ideally $YNbO_4$) has already been mentioned repeatedly: Coomaraswamy (1906) reported that the "*gurupachcha*", found in many localities in Sabaragamuwa, has been identified as fergusonite containing ~2 wt% ThO_2 and >4 wt% UO_2. In a 1977 international uranium resources evaluation report of the International Atomic Energy Agency (national favourability study no. 155) it is stated that intense prospecting of placer deposits in southwestern Sri Lanka had led to identification of several locations of "rare and interesting" minerals, including fergusonite, which however – in contrast to uranothorianite and U- and Th-bearing monazite – are limited in quantity and hence remain of academic interest only (IAEA, 1977). Further occurrences of fergusonite from gem placers in Sabaragamuwa province have been reported by Rupasinghe et al. (1986), Dissanayake and Rupasinghe (1992), Chandrajith et al. (2000) and Dissanayake et al. (2000), but to the best of our knowledge, no detailed mineralogical study of the mineral has been undertaken and published thus far. The aim of the present research is to characterise two fergusonite specimens found in Ratnapura district.

Attention of the readers is drawn on the nomenclature of the mineral. In the present paper, the term "fergusonite" is used to describe a mineral having the composition $YNbO_4$. Fergusonite was named after Robert Ferguson of Raith (1767–1840), a British politician and mineral collector (Haidinger, 1826). However, the plain term fergusonite is actually obsolete and not an accepted name for a mineral species anymore. According to current terminology approved by the Commission on New Minerals,

Nomenclature and Classification of the International Mineralogical Association (IMA–CNMNC), tetragonal $YNbO_4$ (space group $I4_1/a$; also named T phase) is referred to as fergusonite–(Y) [or fergusonite–(Y)–α] whereas monoclinic $YNbO_4$ (space group $I2/a$; M phase) is referred to as fergusonite–(Y)–β. The continuously updated and corrected, complete list of IMA-approved minerals is available at http://cnmnc.main.jp/ (the January 2022 update was accessed on February 7, 2022).

Syntheses and annealing studies have shown that there exists a third polymorph that is also monoclinic (space group $P2/a$; M' phase; Wolten and Chase, 1967; Sugitani and Nagashima, 1975). Both tetragonal fergusonite (Vogt, 1911; Pellas, 1954; Komkov, 1957) and monoclinic fergusonite (Gorshevskaya et al., 1961; Wolten and Chase, 1967; Guastoni et al., 2010) have been reported to occur in nature. In most cases, however, fergusonite is found in a metamict state (Barth, 1926; Mitchell, 1967; Ervanne, 2004; Janeczek, 2004; Gieré et al., 2009; Ruschel et al., 2010). The term metamict, originally introduced by Brøgger (1893), describes a glass-like compound that was initially crystalline but underwent a crystalline-to-aperiodic transition caused by long-lasting radioactive (self-)irradiation (Ewing et al., 1987; Ewing, 1994).

Natural fergusonite and related oxide/niobate minerals have been subject to detailed investigations as petrogenetically important accessory species (Poitrasson et al., 1998; Wang et al, 2003; Gieré et al., 2009) and were considered as potential host materials for the immobilisation of nuclear waste (Cao et al., 2015). Also, synthetic fergusonite-structured compounds are studied as high-performance phosphors (e.g., Hirano and Ishikawa, 2016; Wang et al., 2017; Li et al., 2020).

2. MATERIALS AND METHODS

2.1 Samples

Two Y-Nb-oxide specimens were studied, both originating from Ratnapura district (Fig. 1). The area belongs to the Highland Complex, which is dominated by Proterozoic rocks that have experienced high-grade metamorphism during the Pan-African event ca. 610–520 Ma ago (Cooray, 1994; Kröner et al., 1994; Mathavan and Fernando, 2001).

The first sample, a rounded greyish grain having semi-metallic lustre (ca. 3 cm × 2 cm; Fig. 2), was collected from a placer deposit near Kolonna. It has already been studied by Prame et al. (2014; sample #1 in that study) and was described as "samarskite-group mineral". However, the fact that the Kolonna sample does not contain significant amounts of Fe (Prame et al., 2014) contradicts with the recent redefinition of samarskite-group minerals by Britvin et al. (2019) and hence raises doubts regarding mineral's assignment. Britvin et al. (2019) found that Fe^{3+} (and Mn^{2+}) has a distinct site in the structure of samarskite-group minerals, and they proposed the end-member formula $YFe^{3+}Nb_2O_8$ for samarskite–(Y) (approved by IMA–CNMNC; memorandum 90-FH/18).

The second sample was an elongated, strongly rounded grain (ca. 4 cm × 1.5 cm) of ochre to light brownish colour and non-metallic appearance (Fig. 2). It originates from a quarry near Masimbula, located about 1.5 km southwest of Godakawela. The quarry was operated for gem mining predominantly more than two decades ago. The location is well known for its radioactive minerals (Kuruppu et al., 2020). We may speculate that our sample corresponds to the "radioactive mineral" of Kuruppu et al. (2020; see Fig. 5 in that paper) from the same location, which was suspected as euxenite based on preliminary results of NaI scintillation detector and X-ray diffraction measurements. This identification, however, appears questionable. The mere detection of Ra- and Th-related radioactivity does not help much, as such pattern is obtained from any Th-containing mineral. Broad humps in the X-ray diffraction pattern at d ≈ 2.98 Å and d ≈ 1.77 Å (observed at 2θ angles of 30° and 51.5° when Cu–Kα radiation is used; Kuruppu et al., 2020) cannot be assigned to a crystalline mineral.

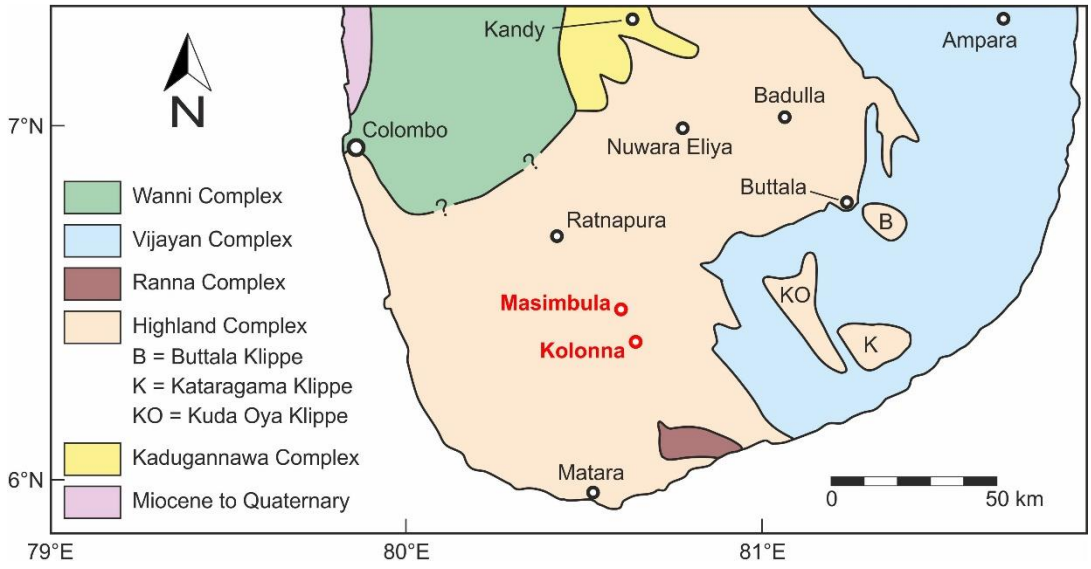

Fig. 1: *Simplified geological map of the southern part of Sri Lanka (modified after Mathavan and Fernando, 2001; Kröner et al., 2013; Nasdala et al., 2017). Fergusonite sampling locations in Ratnapura district, Highland Complex, are highlighted in red*

Rather, these humps are the two characteristic main signals of glassy (that is, metamict) oxides; their detection hence is not of use in mineral identification. Note that X-ray diffraction patterns of metamict euxenite–(Y) (Tomašić et al., 2008), aeschynite–(Y), polycrase–(Y) (Tomašić et al., 2004), samarskite–(Y) (Malczewski et al., 2010), pyrochlore (Zietlow et al., 2017) and fergusonite–(Y) (Tomašić et al., 2006) are widely similar.

2.2 Sample preparation

Samples were cut into slices using a Struers AWS1 abrasive wire saw, and one slice per sample was fractured using a high-alloy steel cylinder and piston (for further details see Nasdala et al., 2018). Another slice per sample was embedded in epoxy, and ground and polished to expose internal textures and features. Doubly polished thin-sections (~25 µm thickness) attached to glass slides were prepared as well. The latter were studied under a polarizing microscope. Both sample mounts and thin-sections were analysed by Raman spectroscopy, and subsequently subjected to obtaining back-scattered electron (BSE) images and conducting electron probe micro-analyser (EPMA) measurements. Prior to the EPMA work, samples were coated with carbon.

For heat-treatment experiments, small chips (0.5–2.0 mm in size) that appeared homogeneous and virtually free of inclusions were selected by screening the fragmented material under a high-magnification binocular microscope. A total of 16 chips per sample were selected. Each of them was then individually placed in a Pt crucible and subjected to dry annealing in air. Samples were heated at a rate of 30 °C min^{-1}. After a 96-hour holding time at the designated temperature (between 200 and 1100 °C), the furnace was switched off and samples remained in the closed furnace until they cooled down to <50 °C. The long, four-day annealing time was chosen to reach near-equilibrium conditions, and slow cooling was chosen to avoid possible build-op of strain during quenching. All 16 chips per sample (one in their natural state and 15 after annealing at different temperatures) were then embedded in epoxy, and ground and polished.

2.3 Analytical details

Mass density was determined hydrostatically by weighing the sample in distilled water (with a drop of detergent to reduce surface tension) and in air. This process was repeated five times.

BSE images were obtained using a Cameca SX100 EPMA. Chemical compositions were determined by means of the same system, operated in wavelength-dispersive X-ray spectrometry (WDS) mode at 15 kV and 20 nA. The electron beam was focused to a 5 µm spot. The following synthetic and natural reference materials were used for calibration (analysed X-ray lines are appended in brackets): albite (Na-Kα), Mg_2SiO_4 (Si-Kα), fluorapatite (P-Kα), sanidine (K-Kα), wollastonite (Ca-Kα), anatase (Ti-Kα), spessartine (Mn-Kα), hematite (Fe-Kα), YAG (Y-Lα), zircon (Zr-Lα), columbite (Nb-Lα), individual $REEPO_4$ (La-Lα, Ce-Lα, Pr-Lβ, Nd-Lβ, Sm-Lα, Eu-Lα, Gd-Lβ, Tb-Lα, Dy-Lβ, Ho-Lβ, Er-Lα, Tm-Lα, Yb-Lα, Lu-Mβ); $CrTa_2O_6$ (Ta-Mα), $CaWO_4$ (W-Mβ), Bi metal (Bi-Mβ), alamosite (Pb-Mβ), ThO_2 (Th-Mα) and UO_2 (U-Mβ). Peak counting times were 10 s for major and 30 s for minor elements; the background counting times were half the respective peak counting times. An X-PHI matrix correction routine (Merlet, 1994) was applied to the raw data. Detection limits of individual elements were calculated using Cameca´s Peaksight software, which is based on the method of Ziebold (1967). Further EPMA experimental details are described elsewhere (Breiter et al., 2009; Škoda et al., 2015).

Raman and laser-induced photoluminescence (PL) spectra were obtained using a Horiba LabRAM HR Evolution spectrometer, equipped with Si-based, Peltier-cooled charge-coupled device detector and Olympus BX-series optical microscope. Raman spectra, and PL emissions in the green to near infrared (NIR) range were excited with the 473 nm emission of a diode-pumped solid-state laser (10 mW at the sample surface). Emissions in the blue range were excited with the ultraviolet (UV) emission of a He-Cd laser (325 nm; 20 mW). The light to be analysed was collected with a 50× objective (numerical aperture 0.55) and dispersed using a diffraction grating with 1800 grooves per millimetre in the optical pathway. Wavenumber calibration was done using the spectrometer´s zero-order line, the Rayleigh line, and emissions of a Kr lamp. For further details, see Zeug et al. (2018).

3. RESULTS AND DISCUSSION

3.1 General characterisation

The two rough samples showed different degrees of weathering. The Kolonna specimen appeared more or less fresh, apart from signs of strong mechanical abrasion, whereas the Masimbula specimen had a thick grey to light brownish weathering crust (Fig. 2) that completely covered the interior's dark colour.

Fig. 2**:** *Fergusonite specimens from Kolonna (left) and Masimbula (right), after being cut in half. Note that upper and lower tips of the Kolonna sample were cut off for analysis during a previous research (Prame et al., 2014)*

After cutting, both samples showed dark greyish brown colour. The rounded shapes of both samples suggest that they have been transported, and deposited, by flowing water. The specific gravity of the Kolonna specimen is 5.5 (Prame et al., 2014) whereas that of the Masimbula specimen is only 4.5. Even though both values lie within the range of specific gravities measured for natural fergusonite [4.3–5.8; http://webmineral.com/data/Fergusonite-(Y).shtml accessed on February 7, 2022], the significant difference between the two values – whose exact reasons remain unclear – is remarkable. It may be speculated that the high degree of chemical alteration in the Masimbula sample may have contributed to this difference. Also, it is known that fluid-driven alteration processes result in porous compounds (Putnis, 2002; Nasdala et al., 2009).

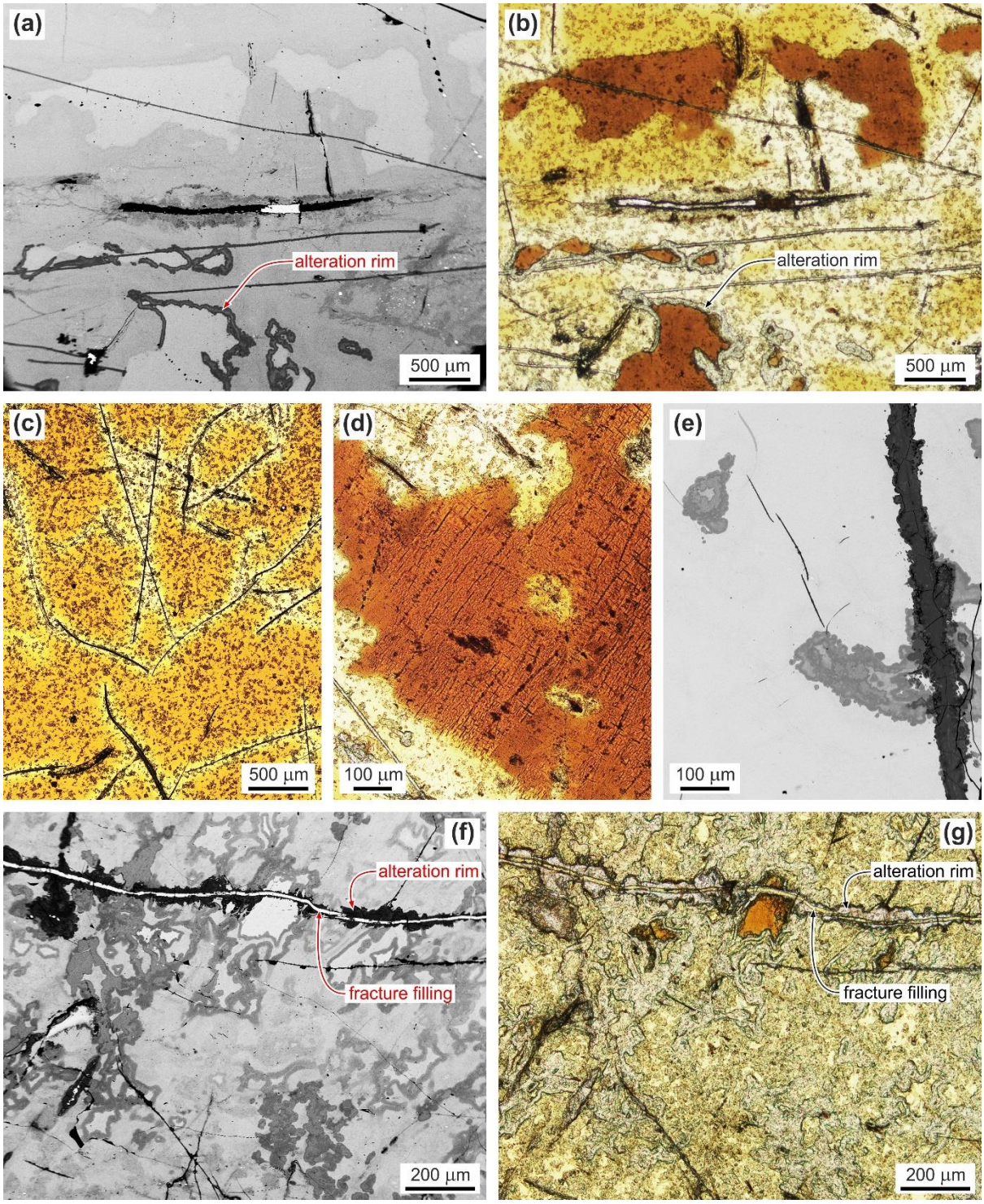

Fig. 3: *Photomicrographs of thin-sections (thicknesses 25 µm) of Kolonna (a–e) and Masimbula (f, g) fergusonite samples. a, e and f are BSE images, and b–d and g are plane-polarised transmitted-light images*

Heavily altered minerals (such as the Masimbula specimen) are therefore expected to have lowered specific gravity. In cross-polarised transmitted light, both samples are nearly isotropic (with the exception of some of the fracture fillings; not shown herein), which suggests their metamict state. Plane-polarized transmitted-light and BSE images (Fig. 3) reveal that both specimens have heterogeneous interiors revealed by rather chaotic BSE-intensity and mineral-colour textures. The degrees of these heterogeneities are different; they are minor in the Kolonna sample (Figs. 3a, b) but extensive in the Masimbula sample (Figs.

3f, g). In transmitted light, both specimens' bulks are light yellow to ochre. In the Kolonna sample, ochre areas appear gradually brightened ("bleached") close to fractures and cracks (Fig. 3c), indicating secondary changes of the chemical composition presumably caused by diffusional processes. The yellow to ochre bulk contains minor, dark brown domains that constitute about 10–30 vol% (Kolonna sample; Fig. 3b) and less than 3 vol% (Masimbula sample, Fig. 3f), respectively. Boundaries among domains are not always sharp but may be rather dull in some cases. The brown domains show slightly higher BSE intensity, compared to their neighbouring ochre areas (see Figs. 3a, b and 3f, g), which is assigned to mild $\bar{Z}$ (i.e., average atomic number) contrast. Brown domains often show a fracture pattern having two angular directions (Fig. 3d). Such pattern might indicate cleavage of a crystalline mineral; however, the brown domains do not yield any interference colours in cross-polarised-light mode (not shown herein) and hence are likely to be metamict. It therefore appears more probable that the fracture pattern indicates either volume shrinking, as could be caused for instance by dewatering, or lower extents of volume expansion (caused by self-irradiation) compared to that of neighbouring domains. Note that more extensive volume expansion in adjacent domains may lead to extensive fracturing of less volume-expanded sample volumes (Chakoumakos et al., 1987).

Along large fractures (Fig. 3f) and at some of the boundaries between brown and ochre domains (Fig. 3b), there are nearly colourless alteration products that have particularly low BSE intensity (Figs. 3a, e). The latter observation strongly supports the interpretation of the colourless material as a product of fluid-driven alteration, as numerous sub-micrometre pores and voids in such phases (Putnis, 2002) lower the electron back-scatter coefficient (Pointer et al., 1988; Nasdala et al., 2009). Central fillings of fractures, in contrast, have yellow colour (Fig. 3g) and particularly high BSE intensity (Fig. 3f), which is assigned to $\bar{Z}$ contrast (that is, elevated incorporation of heavy elements). Similar alteration patterns and features of fergusonite have already been studied and described in detail elsewhere (Gieré et al., 2009; Ruschel et al., 2010).

3.2 Chemical composition

Results of EPMA chemical analyses of the brown domains, yellow to ochre bulks, and low-BSE alteration rims are presented in Table 1. Both brown domains and bulks of the two samples have rather similar chemical compositions. They are mainly composed of Nb_2O_5 (41–45 wt%), Y_2O_3 (23–24 wt%), and relatively high amounts of REE_2O_3 other than Y_2O_3 (15–18 wt%). Based on the EPMA results, the cation-to-oxygen atomic ratios are about 1:2. This corresponds well with the ABO_4 stoichiometry of fergusonite whereas it contradicts the 1:3 stoichiometry of euxenite, $(Nb,Ta,Ti)_2O_6$. In conclusion, both specimens are identified as fergusonite according to their chemical compositions, whereas their possible identity as samarskite (because of insufficient Fe) or euxenite (inapplicable cation-to-oxygen ratio) is excluded.

In fergusonite, the A site is occupied by Y (and substitutes) whereas the B site is occupied by Nb (and substitutes; see Tomašić et al., 2006; Gieré et al., 2009). Based on the assumption of four O atoms per formula unit, the following simplified mineral formulae were calculated for the two specimens:

$(Y_{0.58}\,REE_{0.27}\,M_{A0.14})\,(Nb_{0.91}\,M_{B0.10})\,O_4$
(Kolonna specimen)

$(Y_{0.57}\,REE_{0.20}\,M_{A0.20})\,(Nb_{0.88}\,M_{B0.15})\,O_4$
(Masimbula specimen)

Here, R_{EE} = lanthanide elements; M_A = Ca, Pb, Th, U and M_B = Si, Ti, Zr, Ta, W. Note that especially the A sites in both samples show wide chemical variability (that is, elevated contents of non-formula elements), which is consistent with results of previous fergusonite studies (Tomašić et al., 2006; Gieré et al., 2009; Ruschel et al., 2010).

Time-integrated self-irradiation doses (i.e., alpha-decay-event doses) were calculated according to Murakami et al. (1991), using the present mean concentrations of Th (Kolonna: ~26,300 ppm; Masimbula: ~38,200 ppm) and U (Kolonna: ~52,300 ppm; Masimbula: ~67,800 ppm) and assuming an age of ~550 Ma. The latter assumption was based on ages of other U- and Th-bearing minerals (zircon, ekanite) from the Highland Complex (Kröner et al., 1987;

Nasdala et al. 2004; 2017). Self-irradiation doses of 1.10×10^{20} α/g (Kolonna sample) and 1.44×10^{20} α/g (Masimbula sample), respectively, were calculated. However, the mean concentrations of U, Th and Pb measured in the assumed-to-be-primary brown domains (Table 1) are converted to "chemical ages" (Montel et al., 1996; Suzuki and Kato, 2008) of roughly 900 Ma (Kolonna sample) and 970 Ma (Masimbula sample), respectively.

***Table 1**: Average results of EPMA analyses of the two fergusonite samples*

	Kolonna			**Masimbula**		
Oxide	**Brown domains (n = 6)**	**Yellow to ochre bulk (n = 14)**	**Alteration rims (n = 4)**	**Brown domains (n = 3)**	**Yellow bulk (n = 27)**	**Alteration rims (n = 4)**
Na_2O	0.06 ± 0.15	0.11 ± 0.04	0.19 ± 0.10	0.01 ± 0.01	0.03 ± 0.05	bdl
MgO	bdl	bdl	0.13 ± 0.01	bdl	0.01 ± 0.05	0.04 ± 0.05
Al_2O_3	bdl	bdl	4.78 ± 0.50	bdl	bdl	0.17 ± 0.06
SiO_2	0.26 ± 0.08	0.22 ± 0.07	2.20 ± 0.11	0.33 ± 0.01	0.46 ± 0.21	3.80 ± 0.34
P_2O_5	0.01 ± 0.02	0.01 ± 0.03	0.29 ± 0.05	0.03 ± 0.04	0.02 ± 0.05	0.11 ± 0.14
K_2O	0.01 ± 0.02	bdl	0.30 ± 0.08	0.01 ± 0.02	0.01 ± 0.04	0.13 ± 0.06
CaO	0.74 ± 0.07	0.75 ± 0.12	1.66 ± 0.08	1.28 ± 0.06	1.17 ± 0.22	0.34 ± 0.26
TiO_2	1.42 ± 0.15	1.36 ± 0.16	2.30 ± 0.25	1.46 ± 0.40	1.54 ± 0.58	2.13 ± 0.13
MnO	0.01 ± 0.02	bdl	bdl	0.01 ± 0.03	0.10 ± 0.22	bdl
FeO [a]	bdl	bdl	6.68 ± 0.38	bdl	0.23 ± 0.44	2.02 ± 0.52
Y_2O_3	24.3 ± 0.5	24.4 ± 1.3	0.40 ± 0.13	24.9 ± 0.6	22.6 ± 1.5	1.76 ± 0.67
ZrO_2	0.11 ± 0.09	0.08 ± 0.11	0.10 ± 0.02	0.21 ± 0.03	0.24 ± 0.09	0.36 ± 0.12
Nb_2O_5	44.7 ± 0.3	44.7 ± 0.5	55.8 ± 0.9	44.2 ± 1.1	40.8 ± 2.0	58.6 ± 2.9
La_2O_3	0.01 ± 0.03	0.01 ± 0.03	bdl	0.02 ± 0.03	0.01 ± 0.04	0.07 ± 0.01
Ce_2O_3	0.14 ± 0.05	0.09 ± 0.19	0.27 ± 0.03	0.13 ± 0.10	0.11 ± 0.15	0.29 ± 0.11
Pr_2O_3	0.06 ± 0.12	0.03 ± 0.10	bdl	0.02 ± 0.04	0.01 ± 0.05	0.03 ± 0.03
Nd_2O_3	0.72 ± 0.09	0.69 ± 0.18	bdl	0.31 ± 0.07	0.30 ± 0.11	0.10 ± 0.05
Sm_2O_3	1.04 ± 0.08	0.98 ± 0.19	bdl	0.41 ± 0.04	0.36 ± 0.10	0.09 ± 0.05
Eu_2O_3	0.01 ± 0.03	0.03 ± 0.03	bdl	0.01 ± 0.01	0.01 ± 0.03	bdl
Gd_2O_3	3.80 ± 0.25	3.71 ± 0.33	bdl	1.85 ± 0.14	1.78 ± 0.31	0.31 ± 0.14
Tb_2O_3	0.55 ± 0.05	0.54 ± 0.07	bdl	0.26 ± 0.09	0.24 ± 0.11	0.02 ± 0.02
Dy_2O_3	4.43 ± 0.28	4.17 ± 0.29	bdl	2.61 ± 0.10	2.36 ± 0.32	0.42 ± 0.17
Ho_2O_3	0.94 ± 0.14	0.87 ± 0.14	bdl	0.51 ± 0.04	0.52 ± 0.18	0.04 ± 0.07
Er_2O_3	3.24 ± 0.14	3.14 ± 0.24	bdl	2.54 ± 0.05	2.44 ± 0.14	0.33 ± 0.17
Tm_2O_3	0.47 ± 0.04	0.47 ± 0.07	bdl	0.51 ± 0.06	0.47 ± 0.06	0.07 ± 0.05
Yb_2O_3	2.37 ± 0.18	2.44 ± 0.26	bdl	3.34 ± 0.25	2.98 ± 0.28	0.51 ± 0.18
Lu_2O_3	0.33 ± 0.07	0.30 ± 0.08	bdl	0.52 ± 0.02	0.48 ± 0.10	0.05 ± 0.05
Ta_2O_5	0.72 ± 0.18	0.73 ± 0.10	0.70 ± 0.06	1.40 ± 0.04	1.30 ± 0.19	2.28 ± 0.24
WO_3	0.95 ± 0.18	0.82 ± 0.28	0.17 ± 0.19	1.16 ± 0.13	1.07 ± 0.52	0.59 ± 0.34
PbO	0.88 ± 0.14	0.80 ± 0.26	2.28 ± 0.29	1.24 ± 0.18	1.02 ± 0.32	1.63 ± 0.10
ThO_2	2.87 ± 0.22	2.96 ± 0.53	3.33 ± 0.35	3.27 ± 0.41	4.63 ± 1.21	6.57 ± 1.41
UO_2	5.86 ± 0.34	5.92 ± 0.37	4.96 ± 1.08	7.77 ± 0.34	7.65 ± 0.37	5.05 ± 1.37
Total	101.1 ± 0.9	100.2 ± 1.1	86.5 ± 1.0	100.3 ± 0.9	95.1 ± 3.6	88.3 ± 2.1

Notes: All errors are quoted at the 2σ level. bdl = below the EPMA detection limit
[a] Total Fe is quoted as FeO

Using these "chemical ages", correspondingly higher self-irradiation doses of 1.83×10^{20} α/g (Kolonna sample) and 2.59×10^{20} α/g (Masimbula sample), respectively, were calculated. More precise conclusions will require the conduction of U–Th–Pb geochronology analyses. However, all of these calculated doses are well beyond the critical dose of about 1×10^{19} α/g that is needed to cause metamictisation of Sri Lankan zircon (Zhang et al., 2000; Nasdala et al., 2004). This finding agrees well with the isotropic character of the samples suggesting a glassy state.

Chondrite-normalized plots of lanthanide concentrations (Fig. 4) reveal a general increase from light REEs to medium-to-heavy REEs, which is consistent with results of other studies on this mineral (Giere et al., 2009; Abu Elatta and Mahmoud, 2019; Zozulya et al., 2020). The Eu concentration (Table 1) is extremely low (on the order of the EPMA detection limit) in both specimens, causing strongly negative Eu anomalies (Fig. 4). The Eu/Eu* ratio [with $Eu^* = (Sm \times Gd)^{0.5}$; compare McLennan, 1989] was calculated as 0.03 for the Kolonna sample and 0.04 for the Masimbula sample, respectively. Cerium shows an insignificant behaviour to weakly positive anomaly (Fig. 4). The observation of strong negative Eu anomalies (that concurs well with the absence of strongly positive Ce anomalies) indicates reducing conditions during fergusonite formation (Trail et al., 2012).

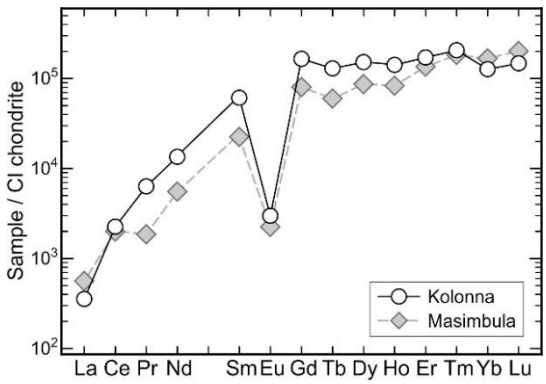

Fig. 4. *Plot of chondrite-normalized REE concentrations in the two fergusonite specimens. Both samples show increases from light REEs to medium and heavy REEs, and significant negative Eu anomalies.*

Chemical compositions of alteration rims (nearly colourless, and characterised by low BSE intensity; Fig. 3) differ notably from that of their host material. Interestingly, there are some observations common to both samples but there are some differences too (Table 1). In general, Si, Fe and Nb concentrations are high, and Ti and Pb are moderately high in the alteration rims, compared to their hosts, whereas the majority of Y as well as significant fractions of other REEs, W, and also some U are lost. The elements Al and Ca are enriched only in the alteration rims in the Kolonna sample whereas alteration of the Masimbula sample has resulted in Ca loss but moderate Th gain. Alteration rims in both samples yielded strongly deficient EPMA analytical totals (Table1), which – in analogy to low electron back-scatter coefficients – is assigned to the porosity of alteration products (Nasdala et al., 2009; and references therein).

The fact that already the yellow bulk of the Masimbula sample yielded (mildly) deficient analytical totals, may point to significant contents of (light) elements that cannot be analysed by the EPMA. However, in view of the rather chaotic and non-primary textures of this sample it appears much more likely that the yellow bulk has already experienced a (rather mild) chemical alteration overprint, with alteration rims and fracture fillings representing either another event or a more intense stage of the chemical alteration. This interpretation is also consistent with the sample's low specific gravity. Consequently, the Masimbula sample represents the product of particularly extensive (and perhaps even multiple) chemical alteration, with the small volume fraction of brownish domains representing the leftover of the primary mineral. The observation that not only the (primary) brown domains but also the alteration products (i.e., both yellow to ochre bulk and near-colourless alteration rims) are isotropic, indicates that the chemical alteration did not occur recently under weathering conditions, but a long time ago already: Alteration products obviously had enough time to become metamict due to extended self-irradiation. Similar internal patterns of chemical alteration in fergusonite have already been described in great detail elsewhere (Ruschel et al., 2010).

3.3 Raman and PL spectroscopy

Representative Raman spectra of unheated samples and their annealing products are presented in Fig. 5. For analysis, 473 nm excitation was preferred because it turned out that with green (532 nm), red (633 nm) and NIR (785 nm) excitation, Raman signals were obscured by laser-induced luminescence. Spectra of the two specimens are widely similar. The un-annealed samples yielded only the broad pattern that is typical of a glassy compound, indicating a metamict state (which is consistent with the absence of birefringence).

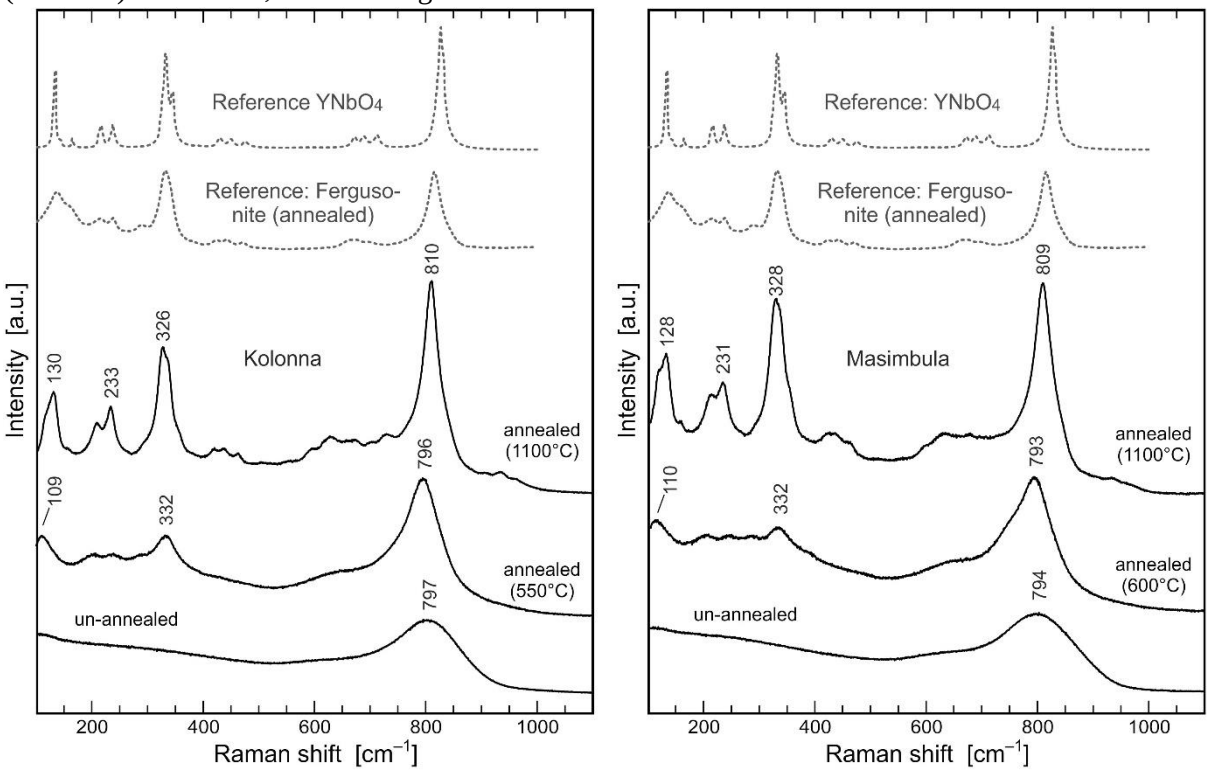

Fig. 5: *Raman spectra (473 nm excitation) of un-annealed samples and their annealed counterparts. The reference spectrum of a fully annealed, previously metamict fergusonite from Berere (Madagaskar) is from Ruschel et al. (2010), and the reference spectrum of synthetic, monoclinic $YNbO_4$ was extracted from Yashima et al. (1997)*

After annealing at 550°C (Kolonna sample) and 600°C (Masimbula sample), respectively, the Raman pattern of tetragonal $YNbO_4$, and after annealing at ≥750°C the Raman pattern of monoclinic $YNbO_4$ is obtained. The latter spectra correspond reasonably well with that of fergusonite–(Y)–β obtained by Tomašić et al. (2006) and Ruschel et al. (2010), and with the spectrum of the monoclinic $YNbO_4$ phase synthesized by Yashima et al. (1997). Note that the latter is assigned to high-temperature tetragonal $YNbO_4$ that underwent tetragonal-to-monoclinic transformation upon cooling to room temperature (Mather and Davies, 1995). The fact that spectra of annealed analogues of natural samples show much wider bands than that of synthetic $YNbO_4$ is explained by "chemical band broadening", that is, extensive contents of non-formula constituents in the natural samples. For band assignment see Blasse (1973).

It should be noted that fergusonite–(Y)–β Raman spectra that are available in the online RRUFF database (https://rruff.info accessed on November 12, 2021; RRUFF ID #R070600 and #R080103) were obtained with 532 and 780 nm excitation. As a consequence, the RRUFF spectra are strongly biased and obscured by intense PL emissions. Their proposed suitability as reference spectra hence appears limited. Doubts regarding the RRUFF spectra are substantiated by the fact that, in spite of the claim "the identification of this mineral has been confirmed by X-ray diffraction", data set

#R070600 actually belongs to xenotime–(Y), not fergusonite–(Y)–β.

Photoluminescence spectra of the Kolonna and Masimbula samples are presented in Fig. 6. Emission in the violet to blue range of the electromagnetic spectrum was obtained using UV and the rest using blue laser excitation. Spectra are widely identical for the two samples; full spectra of the un-annealed and fully annealed material are therefore only shown for the Kolonna specimen. The un-annealed specimens do not show much PL, which is explained by luminescence quenching in strongly radiation-damaged structures (Nasdala et al., 2013).

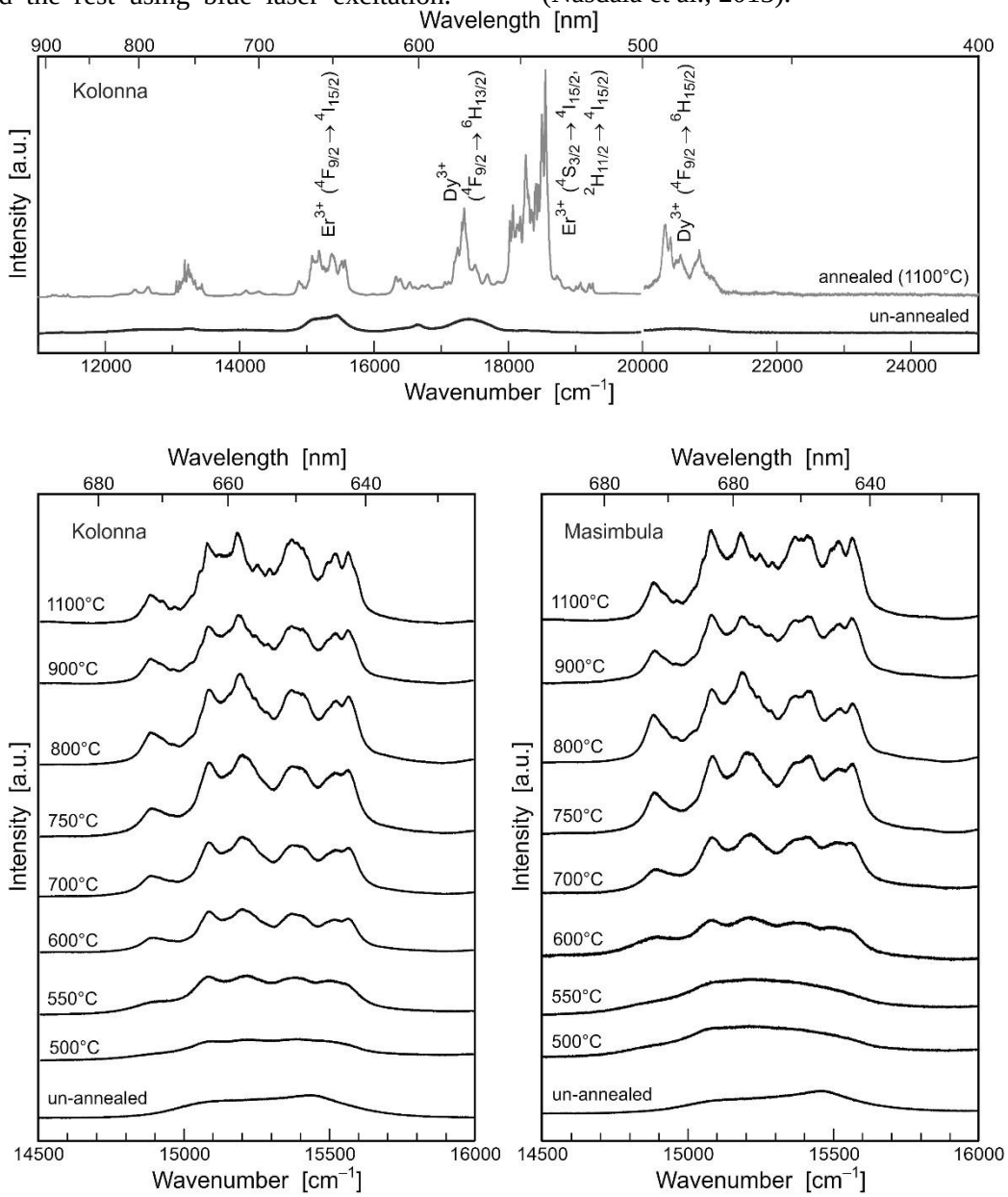

Fig. 6: *Laser-induced PL spectra, shown with vertical offset for clarity. Top, overview spectra of the un-annealed (that is, metamict) Kolonna sample and its fully annealed counterpart (above 20000 cm^{-1} obtained with 325 nm and below 20000 cm^{-1} with 473 nm laser excitation). Below, series of spectra (473 nm excitation) for the two samples, visualising the recovery of the short-range order (seen from the development of the fine-structure) depending on the annealing temperature*

Structural recovery upon annealing leads to a general increase of the emission intensity and crystal-field splitting of electronic transitions into multitudes of so-called Stark lines. The emissions are related to trivalent REEs, especially to Er^{3+} (Wang et al., 2017) and Dy^{3+} (Li et al., 2020).

The fine structure (i.e. splitting into narrow bands) of the 14900–15600 cm^{-1} group of emissions (corresponding to 670–640 nm wavelength) in the red range of the electromagnetic spectrum was selected for monitoring in more detail (i) recrystallization of the metamict material and (ii) $\alpha \rightarrow \beta$ transition. This group of narrow lines is assigned to the $^4F_{9/2} \rightarrow {}^4I_{15/2}$ electronic transition of Er^{3+}, with minor contribution of the $^4F_{9/2} \rightarrow {}^6H_{11/2}$ transition of Dy^{3+} (Wang et al., 2017; Li et al., 2020). In analogy to Raman spectra, recrystallization to form tetragonal $YNbO_4$ is observed at 550°C (Kolonna sample) and 600°C (Masimbula sample), respectively. Transition to monoclinic $YNbO_4$ is observed for samples annealed at 750°C and above. Slight differences of recrystallization and transition temperatures noted in the samples of the present study to those published by Tomašić et al. (2006) and Ruschel et al. (2010) are assigned to differences in chemical compositions and structural states. The latter concerns the possible minor presence of not fully aperiodic material, which could serve as a starting point for epitaxial growth, whereas the recrystallization of glassy material depends on random nucleation.

4. CONCLUSIONS

Both specimens under study are identified as fergusonite that underwent crystalline-to-aperiodic transformation due to extensive self-irradiation over geologic periods of time. However, it cannot be determined whether the primary samples or the material that existed before self-irradiation were tetragonal fergusonite–(Y) or monoclinic fergusonite–(Y)–β. For this reason, we abstain from assigning the primary samples to either "fergusonite–(Y)" or "fergusonite–(Y)–β", which would be purely speculative. Instead, we use the general term fergusonite.

Both samples underwent extensive chemical alteration, which is most likely not related to recent weathering but may have occurred as the result of a (fluid-driven) overprint event. Our observations are consistent with previous findings on this mineral: It is well known that fergusonite, especially when lowered in chemical resistance due to metamictisation, is prone to chemical alteration (Lumpkin, 1998; Ercit, 2005; Ruschel et al., 2010, Škoda et al., 2011, Zozulya et al., 2020).

ACKNOWLEDGEMENTS

The Kolonna sample was obtained from G.D. Nandana Edirisinghe, and the Masimbula sample was provided by Malathunga Arachchige Abeysinghe. Sample preparation was done by Andreas Wagner. Gerald Giester assisted in determining mass density. Nikolay V. Sobolev and Wolfgang Zirbs kindly helped in acquiring literature. Comments by G.W.A. Rohan Fernando and Christoph Hauzenberger are greatly appreciated. We are most grateful to two anonymous experts whose constructive reviews helped to improve the quality of the manuscript. Authors A.E. and L.N. acknowledge travel support from the Faculty of Geosciences, Geography and Astronomy, University of Vienna.

REFERENCES

Abu Elatta, S. and Mahmoud, A. (2019) Geology, mineralogy and mineral chemistry of the NYF-type pegmatites at the Gabal El Faliq area, South Eastern Desert, Egypt. Journal of Earth System Science, 128: 156.

Barth, T. (1926) The structure of synthetic, metamict, and recrystallized fergusonite. Norsk Geologisk Tidsskrift, 9: 23–29.

Blasse, G. (1973) Vibrational spectra of yttrium niobate and tantalite. Journal of Solid State Chemistry, 7: 169–171.

Breiter K., Copjakova R. and Skoda, R. (2009) The involvement of F, CO_2, and As in the alteration of Zr-Th-REE-bearing accessory minerals in the Hora Svate Kateriny A-type granite, Czech Republic. Canadian Mineralogist, 47(6): 1375–1398.

Britvin, S.N., Pekov, I.V., Krzhizhanovskaya, M.G., Agakhanov, A.A., Ternes, B., Schüller, W. and Chukanov, N.V. (2019) Redefinition and crystal chemistry of samarskite-(Y), $YFe^{3+}Nb_2O_8$: cation-ordered niobate structurally related to layered double tungstates. Physics and Chemistry of Minerals, 46(7): 727–741.

Brøgger, W.C.A. (1893) Salmonsens Store Illustrerede Konversationsleksikon 1. Brødrene Salmonsen, Kopenhagen, pp. 742–743.

Cao, Q., Krivovichev, S.V., Burakov, B.E., Liu, X. and Liu, X. (2015) Natural metamict minerals as analogues of aged radioactive waste forms. Journal of Radioanalytical and Nuclear Chemistry, 304(1): 251–255.

Chakoumakos, B.C., Murakami, T., Lumpkin, G.R. and Ewing, R.C. (1987) Alpha-decay-induced fracturing in zircon: The transition from the crystalline to the metamict state. Science, 236: 1556–1559.

Chandrajith, R., Dissanayake, C.B. and Tobschall, H.J. (2000) The stream sediment geochemistry of the Walawe Ganga Basin of Sri Lanka – Implications for Gondwana mineralization. Gondwana Research, 3(2): 189–204.

Coomaraswamy, A.K. (1906) Report of the director of the Mineralogical Survey for 1906. Ceylon Mineral Survey, Administration Report, Part IV, 13 pp.

Cooray, P.G. (1994) The Precambrian of Sri Lanka: A historical review. Precambrian Research, 66: 3–18.

Dissanayake, C.B. and Rupasinghe, M.S. (1992) Application of geochemistry to exploration for gem deposits, Sri Lanka. Journal of Gemmology, 23(3): 165–175.

Dissanayake, C.B., Chandrajith, R. and Tobschall, H.J. (2000) The geology, mineralogy and rare element geochemistry of the gem deposits of Sri Lanka. Bulletin of the Geological Society of Finland, 72(1–2): 5–20.

Ercit, T.S. (2005) Identification and alteration trends of granitic-pegmatite-hosted (Y,REE,U,Th)–(Nb,Ta,Ti) oxide minerals: a statistical approach. Canadian Mineralogist, 43(4): 1291–1303.

Ervanne, H. (2004) Uranium oxidation states in allanite, fergusonite and monazite of pegmatites from Finland. Neues Jahrbuch für Mineralogie / Monatshefte, 2004(7): 289–301.

Ewing, R.C., Chakoumakos, B.C., Lumpkin, G.R. and Murakami, T. (1987) The metamict state. MRS Bulletin, 12(4): 58–66.

Ewing, R.C. (1994) The metamict state: 1993 – the centennial. Nuclear Instruments and Methods in Physics Research, Section B, 91(1–4): 22–29.

Gieré, R., Williams, C.T., Wirth, R. and Ruschel, K. (2009) Metamict fergusonite-(Y) in a spessartine-bearing granitic pegmatite from Adamello, Italy. Chemical Geology, 261(3–4), 333–345.

Gorshevskaya, S.A., Sidorenko, G.A. and Smorchkov, I.E. (1961) A new modification of fergusonite: β-fergusonite. Geologiya Rudnykh Mestorozhdenii, 9: 28–29 (in Russian).

Guastoni, A., Cámara, F. and Nestola, F. (2010) Arsenic-rich fergusonite-beta-(Y) from Mount Cervandone (Western Alps, Italy): Crystal structure and genetic implications. American Mineralogist, 95(4): 487–494.

Haidinger, W. (1826) XIX. Description of fergusonite, a new mineral species. Earth and Environmental Science Transactions of The Royal Society of Edinburgh, 10(2): 271–278.

Hirano, M. and Ishikawa, K. (2016) Intense up-conversion luminescence of Er^{3+}/Yb^{3+} co-doped $YNbO_4$ through hydrothermal route. Journal of Photochemistry and Photobiology A: Chemistry, 316: 88–94.

IAEA (1977) International uranium resources evaluation project. Natural favourability studies #105: Sri Lanka. International Atomic Energy Agency, document 77–9995.

Janeczek, J. (2004) Re-examination of kochelite: a mixture of metamict fergusonite-(Y) and altered zircon. Neues Jahrbuch für Mineralogie / Monatshefte, 2004(5): 193–207.

Komkov, A.I. (1957) On fergusonite. Zapiski Vsesoyuznogo Mineralogicheskogo Obshchestva, 86(4): 432–444 (in Russian).

Kröner, A., Williams, I.S., Compston, W., Baur, N., Vitanage, P.W. and Perera, L.R.K. (1987) Zircon ion microprobe dating of high-grade rocks in Sri Lanka. Journal of Geology, 95: 775–791.

Kröner, A., Kehelpannala, K.V.W. and Kriegsman, L.M. (1994) Origin of compositional layering and mechanism of crustal thickening in the high-grade gneiss terrain of Sri Lanka. Precambrian Research, 66: 21–37.

Kröner, A., Rojas-Agramonte, Y., Kehelpannala, K.V.W., Zack, T., Hegner, E., Geng, H.Y., Wong, J. and Barth, M. (2013) Age, Nd–Hf isotopes, and geochemistry of the Vijayan Complex of eastern and southern Sri Lanka: A Grenville-age magmatic arc of unknown derivation. Precambrian Research, 234: 288–321.

Kuruppu, K.A.D.D.N., Hewathilake, H.P.T.S., Illangasinghe, I.K.M.S.C.K., Ranasinghe, R.A.N.C., Jayasinghe, N. and Dharmaratne, T.S. (2020) Radioactivity survey on Godakawela gem field in Sri Lanka; to identify the origin of the unknown radioactive mineral. Journal of the Geological Society of Sri Lanka, 21(1): 57–65.

Li, Y., Xiao, J., Zhou, Y., Meng, D., Che, A. and Zhao, L. (2020) $YNbO_4:RE^{3+}$ (RE = Eu, Sm, Pr, Dy) phosphors: The luminescence properties and The energy transfer between the host and the RE^{3+} ions. Optik, 208: 164126.

Lumpkin, G.R. (1998) Rare-element mineralogy and internal evolution of the Rutherford #2 pegmatite, Amelia County, Virginia: a classic locality revisited. Canadian Mineralogist, 36(2): 339–353.

Malczewski, D., Grabias, A. and Dercz, G. (2010) ^{57}Fe Mössbauer spectroscopy of radiation damaged samarskites and gadolinites. Hyperfine Interactions, 195(13): 85–91.

Mathavan, V. and Fernando, G.W.A.R. (2001) Reactions and textures in grossular-wollastonite-scapolite calc-silicate granulites from Maligawila, Sri Lanka: Evidence for high-temperature isobaric cooling in the meta-sediments of the Highland Complex. Lithos, 59: 217–232.

Mather, S.A. and Davies, P.K. (1995) Nonequilibrium phase formation in oxides prepared at low temperature: Fergusonite-related phases. Journal of the American Ceramic Society, 78(19): 2737–2745.

McLennan, S.M. (1989) Rare earth elements in sedimentary rocks: Influence of provenance and sedimentary processes. In: Lipin, B.R., McKay, G.A. (eds.) Geochemistry and mineralogy of rare earth elements. Reviews in Mineralogy, vol. 21. Mineralogical Society of America, Washington D.C., pp. 169–200.

Merlet, C. (1994) An accurate computer correction program for quantitative electron probe microanalysis. Mikrochimica Acta, 114/115(1): 363–376.

Mitchell, R.S. (1967): Virginia metamict minerals: X-ray study of fergusonite. Southeastern Geology 8(3): 145–153.

Montel, J.M., Foret, S., Veschambre, M., Nicollet, C. and Provost, A. (1996) Electron microprobe dating of monazite. Chemical Geology, 131(1–4): 37–53.

Murakami, T., Chakoumakos, B.C., Ewing, R.C., Lumpkin, G.R. and Weber, W.J. (1991) Alpha-decay event damage in zircon. American Mineralogist, 76: 1510–1532.

Nasdala, L., Reiners, P.W., Garver, J.I., Kennedy, A.K., Stern, R.A., Balan, E. and Wirth, R. (2004) Incomplete retention of radiation damage in zircon from Sri Lanka. American Mineralogist, 89: 219–231.

Nasdala, L., Kronz, A., Wirth, R., Váczi, T., Pérez-Soba, C., Willner, A. and Kennedy, A.K. (2009) Alteration of radiation-damaged zircon and the related phenomenon of deficient electron microprobe totals. Geochimica et Cosmochimica Acta, 73: 1637–1650.

Nasdala, L., Grambole, D. and Ruschel. K. (2013) Review of effects of radiation damage on the luminescence emission of minerals, and the example of He-irradiated $CePO_4$. Mineralogy and Petrology, 107: 441–454.

Nasdala, L., Corfu, F., Blaimauer, D., Chanmuang, C., Ruschel, K., Škoda, R., Wildner, M., Wirth, R., Zeug, M. and Zoysa, E.G. (2017) Neoproterozoic amorphous "ekanite" ($Ca_2Th_{0.9}U_{0.1}Si_8O_{20}$) from Okkampitiya, Sri Lanka: A metamict gemstone with excellent lead-retention performance. Geology, 45: 919–922.

Nasdala, L., Corfu, F., Schoene, B., Tapster, S.R., Wall, C.J., Schmitz, M.D., Ovtcharova, M., Schaltegger, U., Kennedy, A.K., Kronz, A., Reiners, P.W., Yang, Y.-H., Wu, F.-Y., Gain, S.E.M., Griffin, W.L., Szymanowski, D., Chanmuang N., C., Ende, M., Valley, J.W., Spicuzza, M.J., Wanthanachaisaeng, B. and Giester, G. (2018) GZ7 and GZ8 – two zircon references for SIMS U–Pb geochronology. Geostandards and Geoanalytical Research, 42: 431–457.

Pellas, P. (1954) Sur une fergusonite anisotrope de Naegi (Japon). Bulletin de la Société Française de Minéralogie et de Cristallographie, 77: 461–473.

Pointer C.M., Ashworth J.R. and Ixer, R.A. (1988) The zircon-thorite mineral group in metasomatized granite, Ririwai, Nigeria. 2. Zoning, alteration and exsolution in zircon. Mineralogy and Petrology, 39: 21–37.

Poitrasson, F., Paquette, J.-L., Montel, J.-M., Pin, C. and Duthou, J.-L. (1998): Importance of late-magmatic and hydrothermal fluids on the Sm–Nd isotope mineral systematics of hypersolvus granites. Chemical Geology, 146: 187–203.

Prame, W.K.B.N., Edirisinghe, G.D.N., De Silva, K.T.U.S. and Dissanayake, D.M.S. (2014) Samarskite-polycrase group minerals and other radio-active minerals associated with gem gravels in the Ratnapura gem field of Sri Lanka. In: Proceedings of the Geolological Society of Sri Lanka 30th Technical Session, 1 p.

Putnis, A. (2002) Mineral replacement reactions: from macroscopic observations to microscopic mechanisms. Mineralogical Magazine, 66: 689–708.

Rupasinghe, M.S., Senaratne, A. and Dissanayake, C.B. (1986) Light, heavy and rare minerals in the washed gem gravels of Sri Lanka. Journal of Gemmology, 20(3): 177–184.

Ruschel, K., Nasdala, L., Rhede, D., Wirth, R., Lengauer, C.L. and Libowitzky E. (2010) Chemical alteration patterns in metamict fergusonite. European Journal of Mineralogy, 22(3): 425–433.

Škoda, R., Novák, M. and Cícha, J. (2011) Uranium–niobium-rich alteration products after "písekite", an intimate mixture of Y, REE, Nb, Ta, Ti-oxide minerals from the Obrázek I pegmatite, Písek, Czech Republic. Journal of Geosciences, 56(3): 317–325.

Škoda R., Plášil J., Jonsson E., Čopjaková R., Langhof J. and Galiová M.V. (2015) Redefinition of thalénite-(Y) and discreditation of fluorthalénite-(Y): A re-investigation of type material from the Österby pegmatite, Dalarna, Sweden, and from additional localities. Mineralogical Magazine, 79(4): 965–983.

Sugitani, Y. and Nagashima, K. (1975) Flux growth of $YNbO_4$. Mineralogical Journal, 8: 66–71.

Suzuki, K. and Kato, T. (2008) CHIME dating of monazite, xenotime, zircon and polycrase: Protocol, pitfalls and chemical criterion of possibly discordant age data. Gondwana Research, 14(4): 569–586.

Tomašić, N., Gajović, A., Bermanec, V., Rajić Linarić, M. (2004) Recrystallization of meta-mict Nb–Ta–Ti–REE complex oxides: a coupled X-ray-diffraction and Raman spec-troscopy study of aeschynite-(Y) and polycrase-(Y). Canadian Mineralogist, 42: 1847–1857.

Tomašić, N., Gajović, A., Bermanec, V., Su, D.S., Rajić Linarić, M., Ntaflos, T. and Schlögl, R. (2006) Recrystallization mechanisms of fergusonite from metamict mineral precursors. Physics and Chemistry of Minerals, 33(2): 145–159.

Tomašić, N., Bermanec, V., Gajović, A. and Rajić Linarić, M. (2008) Metamict minerals: an insight into a relic crystal structure using XRD, Raman spectroscopy, SAED and HRTEM. Croatica Chemica Acta., 81(2): 391–400.

Trail, D., Watson, E.B. and Tailby, N.D. (2012) Ce and Eu anomalies in zircon as proxies for the oxidation state of magmas. Geochimica et Cosmochimica Acta, 97: 70–87.

Vogt, T. (1911) Vorläufige Mitteilung über Yttrofluorit, eine neue Mineralspezies aus dem nördlichen Norwegen. Centralblatt für Mineralogie, Geologie und Paläontologie, 2: 373–377.

Wang, R.C., Fontan, F., Chen, X.M., Hu, H., Liu, C.S., Xu, S.J. and de Parseval, P. (2003) Accessory minerals in the Xihuashan Y-enriched granitic complex, southern China: a record of magmatic and hydrothermal stages of evolution. Canadian Mineralogist, 41: 727–748.

Wang, X., Li, X., Cheng, L., Xu, S., Sun, J., Zhang, J., Zhang, X., Yang, X. and Chen, B. (2017) Concentration-dependent spectroscopic properties and temperature sensing of $YNbO_4:Er^{3+}$ phosphors. RSC Advances, 7: 23751–23758.

Wolten, G.M. and Chase, A.B. (1967) Synthetic fergusonites and a new polymorph of yttrium tantalate. American Mineralogist, 52(9–10): 1536–1541.

Yashima, M., Lee, J.-H., Kakihana, M. and Yoshimura, M. (1997) Raman spectral characterization of existing phases in the Y_2O_3–Nb_2O_5 system. Journal of Physics and Chemistry of Solids, 58(10): 1593–1597.

Zeug, M., Nasdala, L., Wanthanachaisaeng, B., Balmer, W.A., Corfu, F. and Wildner, M. (2018) Blue zircon from Ratanakiri, Cambodia. Journal of Gemmology, 36(2): 112–132.

Zhang, M., Salje, E.K.H., Farnan, I., Graeme-Barber, A., Daniel, P., Ewing, R.C., Clark, A.M. and Leroux H. (2000) Metamictization of zircon: Raman spectroscopic study. Journal of Physics: Condensed Matter, 12(8): 1915–1925.

Ziebold, T.O. (1967) Precision and sensitivity in electron probe analysis. Analytical Chemistry, 39: 858–861.

Zietlow, P., Beirau, T., Mihailova, B., Groat, L.A., Chudy, T., Shelyug, A., Navrotsky, A., Ewing, R.C., Schlüter, J., Škoda, R. and Bismayer, U. (2017) Thermal annealing of natural, radiation-damaged pyrochlore. Zeitschrift für Kristallographie – Crystalline Materials, 232(1–3): 25–38.

Zozulya, D. Macdonald, R. and Bagiński, B. (2020) REE fractionation during crystallization and alteration of fergusonite-(Y) from Zr-REE-Nb-rich late- to post-magmatic products of the Keivy alkali granite complex, NW Russia. Ore Geology Reviews, 125: 10369